Numerical Methods in Civil Engineering

Size-dependent buckling analysis of non-prismatic Timoshenko nanobeams made of FGMs rested on Winkler foundation

***M. Soltani*[*], *A. Gholamizadeh*[**]**

ARTICLE INFO

Article history:
Received:
August 2018.
Revised:
October 2018.
Accepted:
November 2018.

Keywords:
Stability Analysis; First-order shear deformation theory; Nonlocal parameter; Functionally graded materials; Elastic foundation

Abstract:

In this article, the buckling behavior of tapered Timoshenko nanobeams made of axially functionally graded (AFG) materials resting on Winkler type elastic foundation is perused. It is supposed that material properties of the AFG nanobeam vary continuously along the beam's length according to the power-law distribution. The nonlocal elasticity theory of Eringen is employed to contemplate the small size effects. Based on the first-order shear deformation theory, the system of nonlocal equilibrium equations in terms of vertical and rotation displacements are derived using the principle of total potential energy. To acquire the nonlocal buckling loads, the differential quadrature method is used in the solution of the resulting coupled differential equations. Eventually, an exhaustive numerical example is carried out for simply supported end conditions to investigate the influences of significant parameters such as power-law index, tapering ratio, Winkler parameter, aspect ratio, and nonlocal parameter on the buckling capacity of AFG Timoshenko nanobeams with varying cross-section supported by uniform elastic foundation.

1. Introduction

Due to advancements in manufacturing processes, smart and innovative materials such as Functionally Graded Materials (FGMs) and laminated composites are usually adopted by engineers to enhance the mechanical responses of different structural elements. FGMs are advanced multi-phase composites with the volume fraction of particles varying continuously and gradually through the thickness or longitudinal direction of the member. FGM is first applied in aerospace structures and fusion reactors as thermal barrier materials. In recent years, the use of FGMs has been increasing in automotive, civil, electronic, optical, and mechanical industries due to their conspicuous characteristics such as elimination or minimization of interfacial stress concentration, thermal resistance, and optimal distribution of weight. Buckling analysis and accurate estimation of stability limit state are the crucial parameters in the design of different structural elements made from homogenous and/or composite materials.

**Corresponding Author: Assistant Professor, Department of civil engineering, University of Kashan, Kashan, Iran, E-mail: msoltani@kashanu.ac.ir*
*** MSc Student in Structural Engineering, Department of Civil Engineering, Faculty of Engineering, Shahr-e-Qods Branch, Islamic Azad University.*

Until now, several investigations are thus performed on stability analysis of components through different types of beam theories. Among them, the Euler-Bernoulli and Timoshenko beam theories are extensively used by scholars to precisely peruse the stability problem of beam members under different circumstances. To analyze the mechanical behavior of long and slender members, the Euler–Bernoulli beam model is frequently used by researchers. Within the frame of the Euler-Bernoulli Theory (EBT), the influence of flexural deformation is only taken into account and the impact of transverse shear deformation is not contemplated. Researchers typically adopt the assumptions of the Timoshenko beam model to resolve the EBT drawbacks and deficiencies, particularly when the beams having a small length-to-depth ratio and is moderately deep. In the context of this theory, the effects of rotatory inertia, transverse shear, and bending deformations are taken into consideration. It should be pointed out that these structures can be applied in small size by following the various higher-order size-dependent continuum theories such as the modified couple stress theory [1], surface energy theory [2], and nonlocal

[DOR: 20.1001.1.23454296.2018.3.2.5.3]
[DOI: 10.29252/nmce.3.2.35]

elasticity theory [3-4]. In the following, a brief literature review is presented to introduce some related studies to these subjects.

The semi-inverse approach has been employed by Elishakoff et al. [5] for the vibration analysis of beams made of axially inhomogeneous materials. In the field of nonlocal differential elasticity methodology, Reddy [6] proposed the analytical solutions for the analysis of deformation, buckling, and vibration of beams by considering different shear deformation theories. Wang et al. [7] perused in detail the flexural vibration problem of nano- and micro beams following the assumptions of the nonlocal elasticity theory of Eringen in conjugate with Timoshenko beam model. Aydogdu [8] took into consideration Eringen's elasticity model and different beam theories to derive a generalized nonlocal beam theory for mechanical analysis of nano-size beams. . A numerical formulation based on the method of differential quadrature was proposed by Civalek and Akgöz [9] to study free vibration characteristics of microtubules based on the Eringen's nonlocal elasticity theory and Euler-Bernoulli beam hypothesis. Using Eringen's nonlocal theory, Danesh et al. [10] deduced the motion equations for the longitudinal vibration of nanorods with tapered cross-section and solved them via the differential quadrature method. According to the nonlocal Timoshenko beam theory, stability analysis of nanotubes embedded in an elastic matrix was also performed by Wang et al. [11]. Also, a finite element formulation was suggested by Eltaher et al. [12, 13] to assess the size effects on mechanical responses of nanobeams made from FG materials following the assumptions of the nonlocal continuum theory. Adopting modified couple stress theory, Akgoz and Civalek [14] surveyed the free vibrational problem of axially functionally graded non-uniform microbeams in the context of Euler-Bernoulli beam model. Through the nonlocal theory along with Timoshenko beam model, the free vibrational analysis of magneto-electro-elastic (MEE) nanobeams was assessed by Ke and Wang [15]. A finite element solution was proposed by Pandeya and Singhb [16] to survey the free vibration behavior of fixed-free nanobeam with varying cross-section. According to Eringen's nonlocal theory and Euler–Bernoulli beam model, nonlinear vibration of AFG nanobeam with tapered section was investigated by Shafiei et al. [17]. Akgoz and Civalek [18] applied higher-order shear deformation microbeams and a modified strain gradient theory to analyze the static bending response of single-walled carbon nanotubes embedded in an elastic medium. Based on the finite strain assumption and first-order shear deformation theory, Ghasemi and Mohandes [19, 20] assessed the nonlinear free vibrational response of laminated composite beams subjected to different sets of boundary conditions using the generalized differential quadrature method. Ebrahim et al. [21-23] performed comprehensive investigations on vibration and buckling analyses of nano-scale FG beams under different circumstances through different beam's theories. Mercan and Civalak [24] analyzed the stability of boron nitride nanotube on the elastic matrix by utilizing a discrete singular convolution technique. By considering the impact of the viscoelastic foundation, Calim [25] studied free and forced vibration of AFG Timoshenko beams. The free vibration and static analyses of different types of structural elements made of FGMs under various circumstances including thermal environment and elastic foundation were comprehensively perused by Lezgy-Nazargah et al. [26-31]. In another work, a finite element formulation for static analysis of nanobeams loaded by a distributed force and supported with the Winkler foundation was established by Demir et al. [32]. Soltani and Mohammadi [33] employed the differential quadrature method to survey the buckling behavior of Euler-Bernoulli nanobeams with exponentially varying cross-section rested on a continuum Winkler-Pasternak foundation. With the help of the power series method, Ghanadiasl [34] inspected the vibrational problem of non-uniform Timoshenko beams having elastically end restrained. Soltani and Asgarian [35] combined the power series approximation and the Rayleigh-Ritz method to assess the free vibration and stability of AFG tapered beam resting on Winkler-Pasternak foundation. Employing modified couple stress theory, Ghasemi and Mohandes [36] formulated an innovative methodology to calculate interlaminar normal and shear stresses of transversely loaded micro and nano composite laminated Timoshenko beam subjected to different end conditions. By taking into account the assumptions of third-order shear deformation theory, Arefi and Civalek [37] inspected the static deformation of cylindrical nanoshells made from functionally graded piezoelectric materials supported by Pasternak's elastic foundation. More recently, Soltani and Asgarian [38] assessed the lateral buckling behavior of web and/or flanges tapered thin-walled beams with axially varying materials subjected to simply-supported end conditions via the differential quadrature method.

The main goal of the current paper is to peruse the impact of Winkler parameter on the nonlocal stability strength of AFG nano-size beam with varying cross-section based on the Timoshenko beam model. To this, the coupled governing differential equations for the vertical and rotation deformations are derived using the Eringen's nonlocal elasticity theory and the energy method. To estimate the buckling characteristics, the methodology of differential quadrature is employed. A comparative example is conducted to validate the present formulations and mathematical solutions. Finally, an exhaustive

[DOR: 20.1001.1.23454296.2018.3.2.5.3]
[DOI: 10.29252/nmce.3.2.35]

illustrative example is performed to assess the influence of significant parameters such as axial gradation of material characteristics, aspect ratio, Eringen's parameter, dimensionless Winkler modulus, and tapering ratio on the normalized buckling load of AFG tapered Timoshenko nano-beams rested on elastic foundation subjected to simply supported end conditions.

2. Theoretical formulation

2.1. Kinematics

Consider a straight beam element of length ***L*** with linear varying cross-section subjected to a constant axial compressive force *P* applied at both ends and supported by a continuum elastic foundation (Fig. 1). To model the interaction between an elastic foundation and beam member, the Winkler-type foundation is used in the current study. This model consists of infinitely closed spaced linear translational springs. Also, the interaction between the vertical springs is not considered. It is also assumed that the beam with rectangular cross-section is made from non-homogeneous material with variable properties along the beam's length. The right-hand Cartesian coordinate system, with O*x* the initial longitudinal axis measured from the left end of the beam and O*y*-axis and Oz are the strong and weak bending axes in the lateral and vertical directions, respectively. Based on the assumptions of first-order shear deformation theory, the axial and the vertical displacement components can be expressed as

$$U(x,y,z) = u_0(x) + z\,\theta(x) \tag{1a}$$

$$W(x,y,z) = w(x) \tag{1b}$$

In these equations, *U* denotes the axial displacement, *W* signifies the vertical displacement (in z-direction), and θ represents the angle of rotation of the cross-section due to bending.

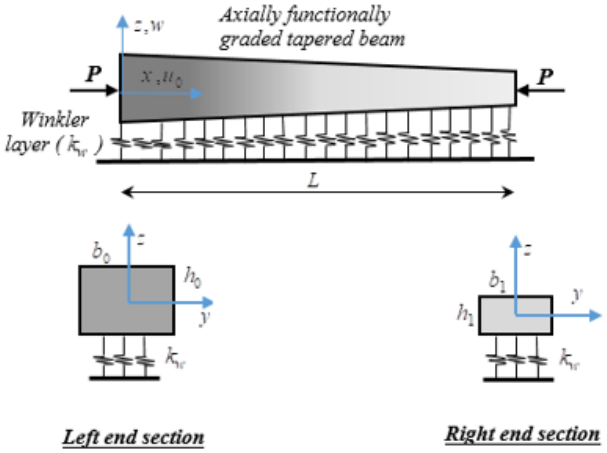

Fig. 1. AFG tapered Timoshenko nanobeam on Winkler's foundation and subjected to an axial load, Coordinate system and notation of displacement parameters

The Green's strain tensor components which incorporate the large displacements and including linear and nonlinear strain parts are given by:

$$\varepsilon_{ij} = \frac{1}{2}\left(\frac{\partial U_i}{\partial x_j} + \frac{\partial U_j}{\partial x_i}\right) + \frac{1}{2}\left(\frac{\partial U_k}{\partial x_i}\frac{\partial U_k}{\partial x_j}\right) = \varepsilon_{ij}^{l} + \varepsilon_{ij}^{*} \qquad i,j,k = x,y,z \tag{2}$$

ε_{ij}^{l} denotes the linear parts and ε_{ij}^{*} the quadratic nonlinear parts. Using the displacement field given in Eq. (1), the non-zero constituents of linear parts of strain-displacement are derived as

$$\varepsilon_{xx}^{l} = \frac{\partial U}{\partial x} = u_0' + z\,\theta' \tag{3a}$$

$$\varepsilon_{xz}^{l} = \frac{1}{2}\left(\frac{\partial U}{\partial z} + \frac{\partial W}{\partial x}\right) = \frac{1}{2}(w' + \theta) \tag{3b}$$

According to the Timoshenko beam hypotheses for small displacements, the non-zero component of nonlinear strain is thus achieved as

$$\varepsilon_{xx}^{*} = \frac{1}{2}\left(\frac{\partial W}{\partial x}\right)^2 = \frac{1}{2}(w')^2 \tag{4}$$

2. 2. Nonlocal elasticity theory

According to the Eringen nonlocal elasticity model [4], the stress at a point inside a body depends not only on the strain state at that point but also on strain states at all other points throughout the body. For homogenous and isotropic elastic solids, the nonlocal stress tensor σ at point *x* can be thus defined as

$$\sigma_{ij}(x) = \int_V \alpha(|x' - x|, \tau) C_{ijkl}\,\varepsilon_{kl}(x')\,dV(x') \tag{5}$$

where ε_{kl} and C_{ijkl} denote the components of linear strain and elastic stiffness coefficients, respectively. Additionally, $\alpha(|x' - x|, \tau)$ is the nonlocal kernel function and $|x' - x|$ is the Euclidean distance. τ stands for material parameter which is defined as $\tau = e_0 a / l$ where *a* is an internal characteristic length (e.g., lattice parameter, C–C bond length, and granular distance) and *l* is an external characteristic length of the nanostructures (e.g., crack length, wavelength). $\boldsymbol{e_0}$ is a material constant that is determined experimentally or approximated by matching the dispersion curves of plane waves with those of atomic lattice dynamics.

It is possible to express the integral constitutive equation presented in Eq. (5) in the form of the following differential constitutive equation:

$$\sigma_{ij} - \mu\nabla^2\sigma_{ij} = C_{ijkl}\,\varepsilon_{kl} \tag{6}$$

where ∇^2 is the Laplacian operator and $\mu = (e_0 a)^2$ denoting the nonlocal parameter. For nanobeam based on the first-

[DOR: 20.1001.1.23454296.2018.3.2.5.3]
[DOI: 10.29252/nmce.3.2.35]

order shear deformation theory, the nonlocal constitutive relations can be written as

$$\sigma_{xx} - \mu \frac{\partial^2 \sigma_{xx}}{\partial x^2} = E\, \varepsilon_{xx}^{l} \tag{7a}$$

$$\sigma_{xz} - \mu \frac{\partial^2 \sigma_{xz}}{\partial x^2} = 2G\, \varepsilon_{xz}^{l} \tag{7b}$$

where E and G are elastic and shear moduli of the beam, respectively. σ_{xx} and σ_{xz} denote the Piola–Kirchhoff stress tensor components.

2. 3. Equilibrium Equations

The principle of minimum total potential energy is adopted herein to obtain equilibrium equations and boundary conditions.

$$\delta\Pi = \delta\left(U_l + U_0 + U_f - W_e\right) = 0 \tag{8}$$

δ illustrates a virtual variation in the last formulation. U_l represents the elastic strain energy, U_0 expresses the strain energy due to the effects of the initial stresses. U_f is the energy corresponding to a uniform elastic foundation and $\boldsymbol{W_e}$ denotes the work of applied loads. For the particular case of linear stability context, where the beam is not under any external force, one considers that the external load work equals to zero.

$$\begin{aligned}\delta\Pi = &\int_0^L \int_A \left(\sigma_{xx}\delta\varepsilon_{xx}^{l} + 2\sigma_{xz}\delta\varepsilon_{xz}^{l}\right)dA\,dx \\ &+\int_0^L \int_A \left(\sigma_{xx}^{0}\delta\varepsilon_{xx}^{*}\right)dA\,dx + \int_0^L \left(k_w w\,\delta w\right)dx\end{aligned} \tag{9}$$

in which $\boldsymbol{L}$ and $\boldsymbol{A}$ express the element length and the cross-sectional area, respectively. ($\delta\varepsilon_{xx}^{l}$, $\delta\varepsilon_{xz}^{l}$) and $\delta\varepsilon_{xx}^{*}$ are the variation of the linear and the nonlinear parts of the strain tensor, respectively. k_w denotes Winkler's foundation constant per unit length of the beam. σ_{xx}^{0} is the initial normal stress in the cross-section, associated with constant axial force ($\boldsymbol{P}$):

$$\sigma_{xx}^{0} = -\frac{P}{A} \tag{10}$$

Substituting equations (3-4) and (10) into relation (9), the expression of the virtual potential energy can be carried out as:

$$\begin{aligned}\delta\Pi = &\int_0^L \int_A \sigma_{xx}\left(\delta u_0' + z\,\delta\theta'\right)dA\,dx \\ &+\int_0^L \int_A \sigma_{xz}\left(\delta w' + \delta\theta\right)dA\,dx \\ &+\int_0^L \int_A \left(-\frac{P}{A}(w'\delta w')\right)dA\,dx + \int_0^L \left(k_w w\,\delta w\right)dx = 0\end{aligned} \tag{11}$$

The variation of strain energy can be formulated in terms of section forces acting on the cross-sectional contour of the elastic member in the buckled configuration. The section stress resultants are presented by the following expressions:

$$N = \int_A \sigma_{xx}\, dA \tag{12a}$$

$$M = \int_A \sigma_{xx}\, z\, dA \tag{12b}$$

$$Q = \int_A \sigma_{xz}\, dA \tag{12c}$$

where $\boldsymbol{N}$ is the axial force applied at the end member. $\boldsymbol{M}$ denotes the bending moments about the major axis. $\boldsymbol{Q}$ is the shear force at any point in the beam. In this stage, by integrating Eq. (11) over the cross-sectional area of the beam and using relations (12a)–(12c), the final form of the variation of total potential energy (δIT) is acquired as:

$$\begin{aligned}\delta\Pi = &\int_L \left(N\,\delta u_0' + M\,\delta\theta'\right)dx + \int_L \left(Q\left(\delta w' + \delta\theta\right)\right)dx \\ &-\int_L \left(P(w'\delta w')\right)dx + \int_0^L \left(k_w w\,\delta w\right)dx = 0\end{aligned} \tag{13}$$

According to the equation presented above, the first variation of total potential energy contains the virtual displacements ($\delta u_0, \delta w, \delta\theta$) and their derivatives. After some calculations and needed simplifications, the following equilibrium equations in the stationary state are obtained:

$$-N' = 0 \tag{14a}$$

$$(Pw')' - Q' + k_w w = 0 \tag{14b}$$

$$-M' + Q = 0 \tag{14c}$$

Under the following boundary conditions:

$$N = 0 \quad \text{Or} \quad \delta u_0 = 0 \tag{15a}$$

$$-Pw' + Q = 0 \quad \text{Or} \quad \delta w = 0 \tag{15b}$$

$$M = 0 \quad \text{Or} \quad \delta\theta = 0 \tag{15c}$$

By substituting Eq. (4a-c) into Eq. (9) and the subsequent results into Eq. (14), the stress resultants are obtained as

$$N - \mu \frac{\partial^2 N}{\partial x^2} = \mathrm{E}A u_0' \tag{16a}$$

$$M - \mu \frac{\partial^2 M}{\partial x^2} = \mathrm{E}I\,\theta' \tag{16b}$$

$$Q - \mu \frac{\partial^2 Q}{\partial x^2} = kGA(w' + \theta) \tag{16c}$$

In previous expressions, k is the shear correction factor and $\boldsymbol{I}$ denotes the moment of inertia. This study is established in the context of small displacements and deformations. According to linear stability, nonlinear terms are also disregarded in the equilibrium equations. Based on these assumptions, the system of stability equations for tapered AFG Timoshenko nanobeam via nonlocal theory is finally derived by replacing Eq. (16) into Eq. (14).

$$\begin{aligned}\delta w \;:\; &\left(kGA(w' + \theta)\right)' - Pw'' + \mu P w^{iv} \\ &-k_w w + \mu k_w w'' = 0\end{aligned} \tag{17a}$$

[DOR: 20.1001.1.23454296.2018.3.2.5.3]
[DOI: 10.29252/nmce.3.2.35]

$$\delta\theta:\ \left(EI\,\theta'\right)' - kGA(w'+\theta) = 0 \qquad (17b)$$

It is necessary to note that the equilibrium equations of local Timoshenko beam resting on elastic foundation are acquired by setting μ=0. The related boundary conditions at the ends of Timoshenko nanobeam can be expressed as

$$N = 0 \quad \text{Or} \quad \delta u_0 = 0 \qquad (18a)$$

$$kGA(w'+\theta) - Pw' + \mu(Pw''' + k_w w') = 0 \quad \text{Or} \quad \delta w = 0 \qquad (18b)$$

$$EI\,\theta' + \mu(Pw'' + k_w w) = 0 \quad \text{Or} \quad \delta\theta = 0 \qquad (18c)$$

In the following section, a numerical solution procedure of the governing equations for flexural-torsional buckling of AFG nanobeam having variable cross-section supported by Winkler foundation is presented based on the differential quadrature method (DQM).

3. Solution Methodology

In the present paper, to solve these differential equations and estimate the axial buckling loads, the differential quadrature method (DQM) is employed. Based on this mathematical method, the displacement components and their relative derivatives are expressed using Lagrange interpolation shape functions [39]. According to DQM, the m^{th}-order derivative of a function *f(x)* is described as

$$\left.\frac{d^m f}{dx^m}\right|_{x=x_p} = \sum_{j=1}^{N} A_{ij}^{(m)} f(x_j) \quad for \quad i = 1,2,...,N \qquad (19)$$

where N is the number of grid points along the x-direction. x_j signifies the position of each sample point and $f(x_j)$ is function values at grid points x_j (i = 1,2,…,N). In this study, Chebyshev–Gauss–Lobatto approach is used to define the position of each sample point

$$x_i = \frac{L}{2}\left[1 - \cos\left(\frac{i-1}{N-1}\pi\right)\right], \quad i = 1,2,...,N \qquad (20)$$

Moreover, $A_{ij}^{(m)}$ denotes the weighting coefficient for the m^{th}-order derivative. The first-order derivative weighting coefficient ($A_{ij}^{(1)}$) is computed by the following algebraic formulations which are based on Lagrange interpolation polynomials:

$$A_{ij}^{(1)} = \begin{cases} \dfrac{M(\xi_i)}{(\xi_i - \xi_j)M(\xi_j)} & for\ \ i \neq j \\ -\displaystyle\sum_{k=1,k\neq i}^{N} A_{ik}^{(1)} & for\ \ i=j \end{cases} \qquad i,j = 1,2,...,N \qquad (21)$$

where

$$M(\xi_i) = \prod_{j=1,j\neq i}^{N} (\xi_i - \xi_j) \quad for \quad i = 1,2,...,N \qquad (22)$$

The higher-order DQM weighting coefficients can be acquired from the first-order weighting coefficient as

$$A_{ij}^{(m)} = A_{ij}^{(1)} A_{ij}^{(m-1)} \qquad 2 \le m \le N-1 \qquad (23)$$

To facilitate the solution of the stability equations utilizing the differential quadrature approach, a non-dimensional variable ($\xi = x/L$) is introduced. By the expansion of Eqs. (17a) - (17b), and then applying the differential quadrature discretization to the non-dimensional form of the resultant equations, the following expressions are obtained:

$$\begin{aligned} &L^2k\,(G(\xi_j)A'(\xi_j)+G(\xi_j)A'(\xi_j))(\sum_{j=1}^{N} A_{ij}^{(1)} w_j) \\ &+L^2kG(\xi_j)A(\xi_j)(\sum_{j=1}^{N} A_{ij}^{(2)} w_j) \\ &+L^3k\,(G(\xi_j)A'(\xi_j)+G'(\xi_j)A(\xi_j))\phi_j \\ &+L^3kG(\xi_j)A(\xi_j)(\sum_{j=1}^{N} A_{ij}^{(1)} \phi_j) \\ &-L^2P(\xi_j)(\sum_{j=1}^{N} A_{ij}^{(2)} w_j) + \mu P(\xi_j)(\sum_{j=1}^{N} A_{ij}^{(4)} w_j) \\ &-L^4k_w w_j + \mu L^2 k_w (\sum_{j=1}^{N} A_{ij}^{(2)} w_j) = 0 \end{aligned} \qquad (24a)$$

$$\begin{aligned} &E(\xi_j)I(\xi_j)(\sum_{j=1}^{N} A_{ij}^{(2)} \phi_j) \\ &+(E(\xi_j)I'(\xi_j)+E'(\xi_j)I(\xi_j))(\sum_{j=1}^{N} A_{ij}^{(1)} \phi_j) \\ &-LkG(\xi_j)A(\xi_j)(\sum_{j=1}^{N} A_{ij}^{(1)} w_j) \\ &-L^2kG(\xi_j)A(\xi_j)\phi_j = 0 \end{aligned} \qquad (24b)$$

It is possible to express the quadrature analog of the mentioned above formulations in the following matrix form:

$$\left(\begin{bmatrix} [K_{\phi\phi}] & [K_{\phi w}] \\ [K_{w\phi}] & [K_{ww}] \end{bmatrix}_{2N\times 2N} - P\begin{bmatrix} [0] & [0] \\ [0] & [K_{G_{ww}}] \end{bmatrix}_{2N\times 2N} + \begin{bmatrix} [0] & [0] \\ [0] & [K_{S_{ww}}] \end{bmatrix}_{2N\times 2N}\right) \times \begin{Bmatrix} \{\phi\} \\ \{w\} \end{Bmatrix}_{2N\times 1} = \begin{Bmatrix} \{0\} \\ \{0\} \end{Bmatrix}_{2N\times 1} \qquad (25)$$

where

$$[K_{\phi\phi}] = [a][A]^{(2)} + [b][A]^{(1)} - L^2k[c] \qquad (26a)$$

$$[K_{\phi w}] = -Lk[c][A]^{(1)} \qquad (26b)$$

$$[K_{ww}] = L^2k([c][A]^{(2)} + [d][A]^{(1)}) \qquad (26c)$$

$$[K_{w\phi}] = L^3k([c][A]^{(1)} + [d]) \qquad (26d)$$

$$[K_{G_{ww}}] = (L^2[A]^{(2)} - \mu[A]^{(4)}) \quad (26e)$$

$$[K_{S_{ww}}] = -L^4[k] + \mu L^2[k][A]^{(2)} \quad (26f)$$

in which

$$a_{jk} = (\mathrm{E}I|_{\xi=\xi_j})\delta_{jk} \quad (27a)$$

$$\mathrm{b}_{jk} = ((\mathrm{E}I' + \mathrm{E}'I)\Big|_{\xi=\xi_j})\delta_{jk} \quad (27b)$$

$$c_{jk} = (GA|_{\xi=\xi_j})\delta_{jk} \quad (27c)$$

$$d_{jk} = ((GA' + G'A)|_{\xi=\xi_j})\delta_{jk} \quad (27d)$$

$$\mathrm{k}_{jk} = (k_w|_{\xi=\xi_j})\delta_{jk} \quad (27e)$$

Here, δ_{jk} is Kronecker delta and defined as

$$\delta_{jk} = \begin{cases} 0 & if\ j \neq k; \\ 1 & if\ j = k. \end{cases} \quad (28)$$

In Eq. (30), the displacement vectors and the torsion angle vector are expressed as:

$$\{w\}_{N\times 1} = \{w_1 \quad w_2 \quad ... \quad w_N\}^T \quad (29a)$$

$$\{\phi\}_{N\times 1} = \{\phi_1 \quad \phi_2 \quad ... \quad \phi_N\}^T \quad (29b)$$

The simple form of the final equation (Eq. (25)) can be stated as

$$\left([K] - \lambda[K_G] + [K_S]\right)_{2N\times 2N} \{d\}_{2N\times 1} = \{0\}_{2N\times 1} \quad (30)$$

in which

$$\{d\} = \begin{Bmatrix} \{\phi\} \\ \{w\} \end{Bmatrix} \quad (31)$$

K, K_G, and K_S are $2N \times 2N$ matrices. As mentioned previously, N denotes the number of grid points along with Under these assumptions, the cross-sectional area $A(x)$ and the area moment of inertia $I(x)$ vary along the beam as

$$A(x) = A_0(1 - \beta x / L)^2;\ I(x) = I_0(1 - \beta x / L)^4 \quad (32)$$

where A_0 and I_0 are respectively cross-sectional area and moment of inertia at the left support ($x=0$). They are defined as: $I_0 = b_0 h_0^3 / 12$ and $A_0 = b_0 h_0$.

It is also contemplated that the beam is made of axially varying materials. The material features vary along the beam's length from pure ceramic at the left end to pure metal at the right one using the simple power-law function, hence, modulus of elasticity can be expressed as:

$$E(x) = E_0 + (E_1 - E_0)(x / L)^m \quad (33)$$

It should be stated that the power-law index (m) is a positive parameter and by setting it equals zero, the tapered beam becomes a fully metal member. It is necessary to note that Poisson's ratio of the material remains constant in the longitudinal direction.

In the numerical computation, the non-dimensional forms of buckling load and elastic foundation parameter are introduced as

$$P_{nor} = \frac{P_{cr} L^2}{E_0 I_0} \qquad \bar{k_w} = k_w \frac{L^4}{E_0 I_0} \quad (34)$$

4.1. Verification

The aim of the first part of the current section is to define the needed number of points along the longitudinal direction while using DQM to obtain an acceptable accuracy on critical elastic buckling loads. Regarding this, Table 1 gives the first non-dimensional buckling load parameters (P_{nor}) of the simply supported prismatic Timoshenko beams ($\boldsymbol{L/b_0}$**=20**) with non-local theory. The convergence study is carried out for various values of the nonlocal parameter. The effects of the number of sampling

the computation domain ($0 \le \xi \le 1$). λs are the eigenvalues and $\{d\}$s are the related eigenvectors. After implementation of the boundary conditions at two ends, not only the buckling loads are computed from the eigenvalue solutions of Eq. (30), but also the vertical deflection and the rotation angle of the AFG Timoshenko nanobeam with varying sections can be determined.

4. Numerical Example

In the current section, an exhaustive example is presented to peruse the influence of axial variation of material properties, tapering ratio, nonlocal parameter, aspect ratio, and elastic foundation modulus on nonlocal stability strength of the simply supported AFG Timoshenko nanobeam with variable cross-section rested on the Winkler foundation. We use the subscripts of $()_0$ and $()_1$ to express the mechanical specifications including the material and geometrical ones of the beam element at the left support ($x=0$, $\xi=0$) and the right one ($x=L$, $\xi=1$), respectively.

Through this numerical example, the linear buckling analysis is performed for a double tapered beam with rectangular cross-section subjected to simply supported end conditions. In this regard, it is supposed that the breadth (b_0) and the height (d_0) of the cross-section at the left end are respectively made to decrease linearly to $b_1 = (1-\beta)b_0$ and $d_1 = (1-\beta)d_0$ at the right one with the same tapering ratio. The tapering ratio is thus defined as $\beta = 1 - b_1/b_0 = 1 - d_1/d_0$. Note that the tapering parameter (β) is a non-negative variable and can change in the range of 0.0 to 0.9. Moreover, by equating this parameter (β) to zero, a uniform beam is achieved.

[DOR: 20.1001.1.23454296.2018.3.2.5.3]
[DOI: 10.29252/nmce.3.2.35]

points used in DQM on convergence are also displayed in Table 1. The obtained results by the proposed numerical technique have been compared with the closed-form solution introduced by Reddy [6]. It is seen from Table 1 that twenty number of grid points (N=20) are sufficient to obtain the lowest buckling load parameters for different nonlocal parameters with the desired accuracy.

Table 1: Convergence of the differential quadrature technique in the determination of the lowest non-dimensional critical buckling load parameters (P_{nor}) for uniform Timoshenko beam with different non-local parameters

(μ)	DQM					Reddy [6]
	Number of points along the x-direction					
	5	10	15	20	30	
0.0	9.7617	9.8067	9.8067	9.8067	9.8067	9.8067
0.5	9.2463	9.3455	9.3455	9.3455	9.3455	9.3455
1	8.7888	8.9257	8.9258	8.9258	8.9258	8.9258
1.5	8.3790	8.5421	8.5421	8.5421	8.5421	8.5421
2.0	8.0093	8.1900	8.1900	8.1900	8.1900	8.1900
2.5	7.6736	7.8658	7.8659	7.8659	7.8659	7.8659
3.0	7.3671	7.5663	7.5664	7.5664	7.5664	7.5664
3.5	7.0859	7.2888	7.2889	7.2889	7.2889	7.2889
4.0	6.8267	7.0309	7.0310	7.0310	7.0310	7.0310
4.5	6.5870	6.7907	6.7907	6.7907	6.7907	6.7907
5.0	6.3646	6.5663	6.5663	6.5663	6.5663	6.5663

In the next step, the validation of the present formulation for buckling analysis of AFG tapered Timoshenko beam supported by elastic foundation within the frame of classic elasticity theory is checked by comparing the archived results with those obtained using finite element formulation developed by Soltani [40]. In this regard, the lowest dimensionless critical loads estimated via DQM with 20 sampling points are arranged in Table 2 for different values of the slenderness ratio (L/b_0) and Winkler parameter ($\bar{k}_w$) at β=0.2. These results are also carried out for two cases: axially non-homogeneous and homogeneous beams. In the case of axially FG members, the distribution of modulus of elasticity is contemplated to vary in the longitudinal direction with a power-law formulation as expressed in Eq. (33). In this case, the material non-homogeneity parameter (***m***) is assumed to be equal to 1. In order to make comparisons possible with Soltani [40], it is assumed that the functionally graded beam is composed of Zirconium dioxide (ZrO_2) and Aluminum (Al) with the following properties (ZrO_2: E0=200GPa; *Al*: E1=70GPa). Also, Table 2 includes the percentage of relative errors (Δ (%)) which are obtained using:

$$\Delta = \left| P_{nor}^{DQM} - P_{nor}^{Ref} \right| / P_{nor}^{Ref} \times 100 \qquad (35)$$

Table 2: Comparison of non-dimensional critical load (P_{nor}) for the local tapered Timoshenko beams for different values of non-homogeneity index (m) and Winkler parameter ($\bar{k}_w$) with the results presented in [40]

Material	L/b_0	$\bar{k}_w = 0$			$\bar{k}_w = 40$			$\bar{k}_w = 80$		
		Present solution	**Soltani [40]**	**Δ (%)**	**Present solution**	**Soltani [40]**	**Δ (%)**	**Present solution**	**Soltani [40]**	**Δ (%)**
Pure Ceramic	5	5.8715	5.8342	0.639	9.8746	9.8243	0.512	13.8425	13.7806	0.449
	10	6.2097	6.1894	0.328	10.2207	10.1952	0.250	14.2106	14.1805	0.212
	50	6.3177	6.3120	0.090	10.3301	10.3228	0.071	14.3242	14.3151	0.064
	100	6.3177	6.3159	0.028	10.3296	10.3269	0.026	14.3228	14.3194	0.024
m=1	5	3.5461	3.5125	0.956	7.2867	7.2245	0.861	10.4373	10.3464	0.878
	10	3.8132	3.7852	0.740	7.6416	7.5997	0.551	11.2431	11.1608	0.737
	50	3.8863	3.8804	0.152	7.7316	7.7214	0.132	11.3933	11.3714	0.193
	100	3.8880	3.8834	0.118	7.7338	7.7252	0.111	11.3969	11.3777	0.169

The efficiency and performance of the adopted mathematical methodology are then confirmed by contrasting the obtained results with those presented in Table 2. For both cases, the values of relative error continually make smaller as the aspect ratio increases.

4.2. Parametric Study

After the validation process of the present formulation for local Timoshenko beam with axially varying material and geometrical properties resting on Winkler foundation subjected to simply supported end conditions, the impacts of different parameters such as material gradient, Winkler's parameter, tapering ratio, aspect ratio, and nonlocality parameter on the critical buckling load of AFG tapered Timoshenko nanobeam are studied. Note that in this section, the AFG beam is made of Alumina (***Al_2O_3***) and Aluminum (***Al***) with the following properties (Al_2O_3*: E_0=380GPa; Al: E_1=70GPa*).

The influence of Eringen's nonlocal parameters (ranging from 0 to 4) on the variations of the non-dimensional normalized buckling loads (P_{nor}) of Timoshenko nanobeam with tapered section made of homogenous materials and axially functionally ones with different

[DOR: 20.1001.1.23454296.2018.3.2.5.3]
[DOI: 10.29252/nmce.3.2.35]

gradient indexes (m=0.6, 1.3 and 2) with respect to tapering ratios (varying from 0 to 0.9) is plotted in Figs. 2-3 for the two different aspect ratios: L/b_0=**20** and L/b_0=**100.**

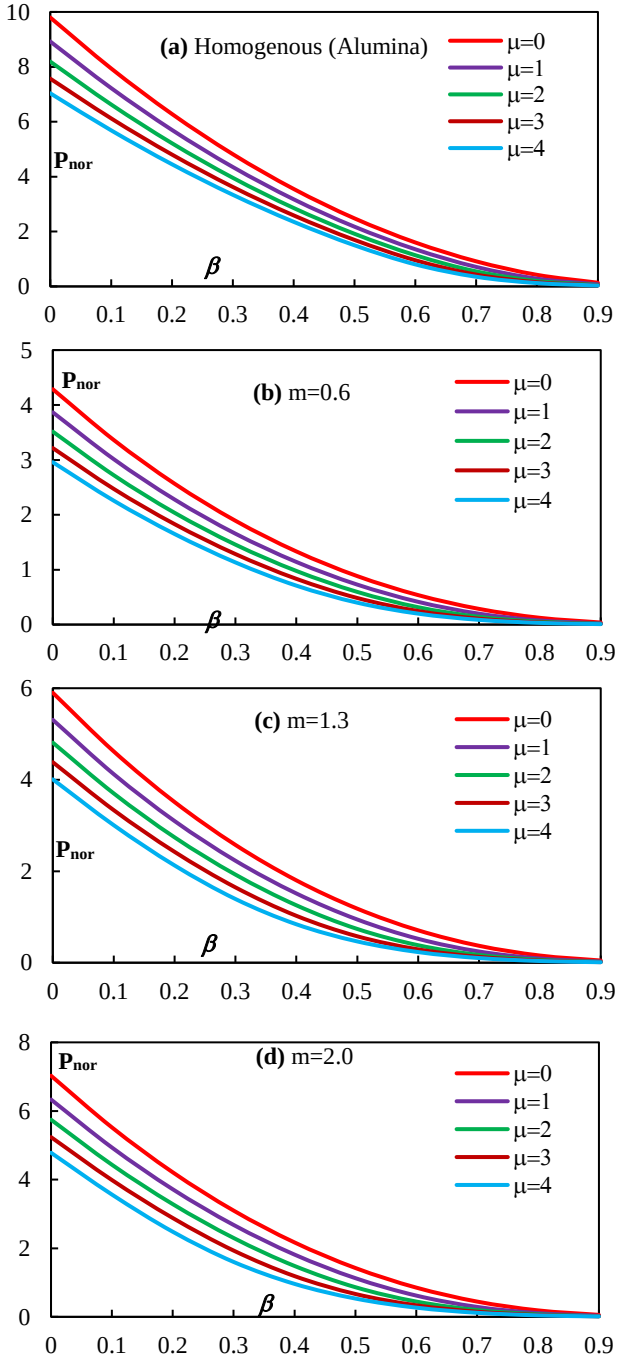

Fig. 2: Variation of the non-dimensional buckling load (P_{nor}) of Timoshenko nanobeam with tapering parameter and nonlocality parameters for different material indexes (L/b_0=**20**).

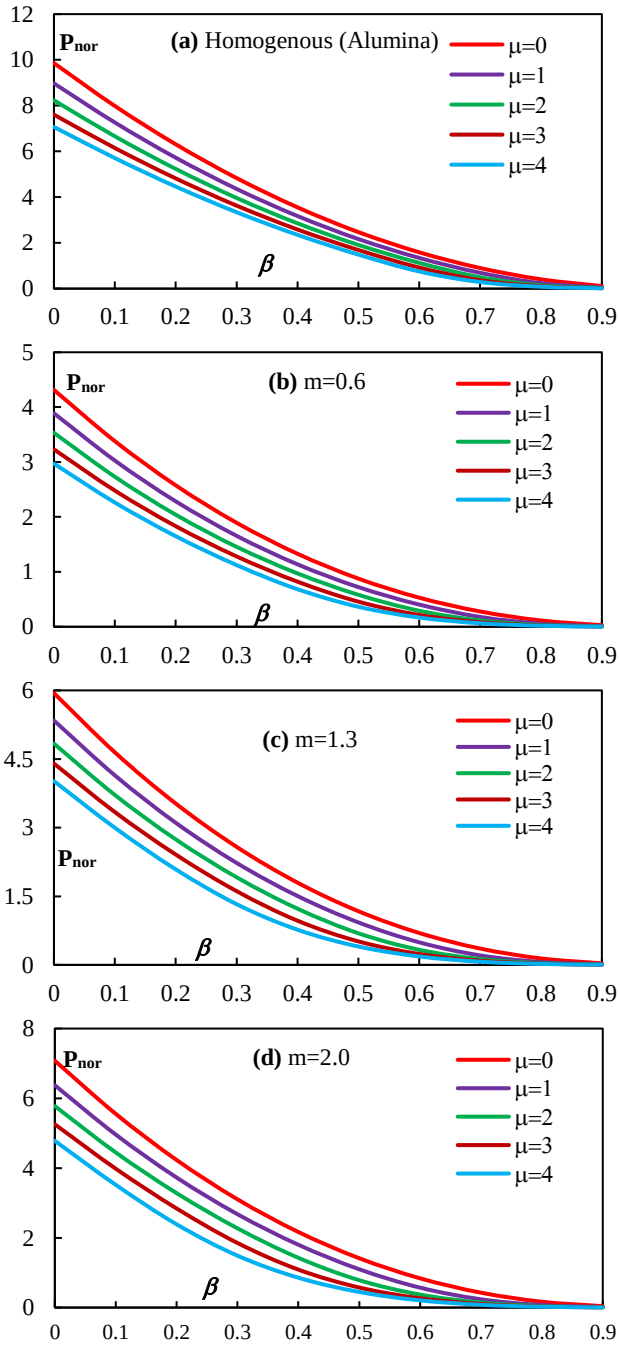

Fig. 3: Variation of the non-dimensional buckling load (P_{nor}) of Timoshenko nanobeam with tapering parameter and nonlocality parameters for different material indexes (L/b_0=**100**).

Subsequently, the lowest non-dimensional buckling load (P_{nor}) variations versus the tapering ratio for different values of gradient indexes (m) and nonlocality parameters (μ=0, 1, 2, and 3) for L/b_0=**10**, are presented in Fig. 4. Each of the depictions of this figure illustrates five different plots relating to m=0.5, 1, 1.5, 2, and 2.5.

[DOR: 20.1001.1.23454296.2018.3.2.5.3]
[DOI: 10.29252/nmce.3.2.35]

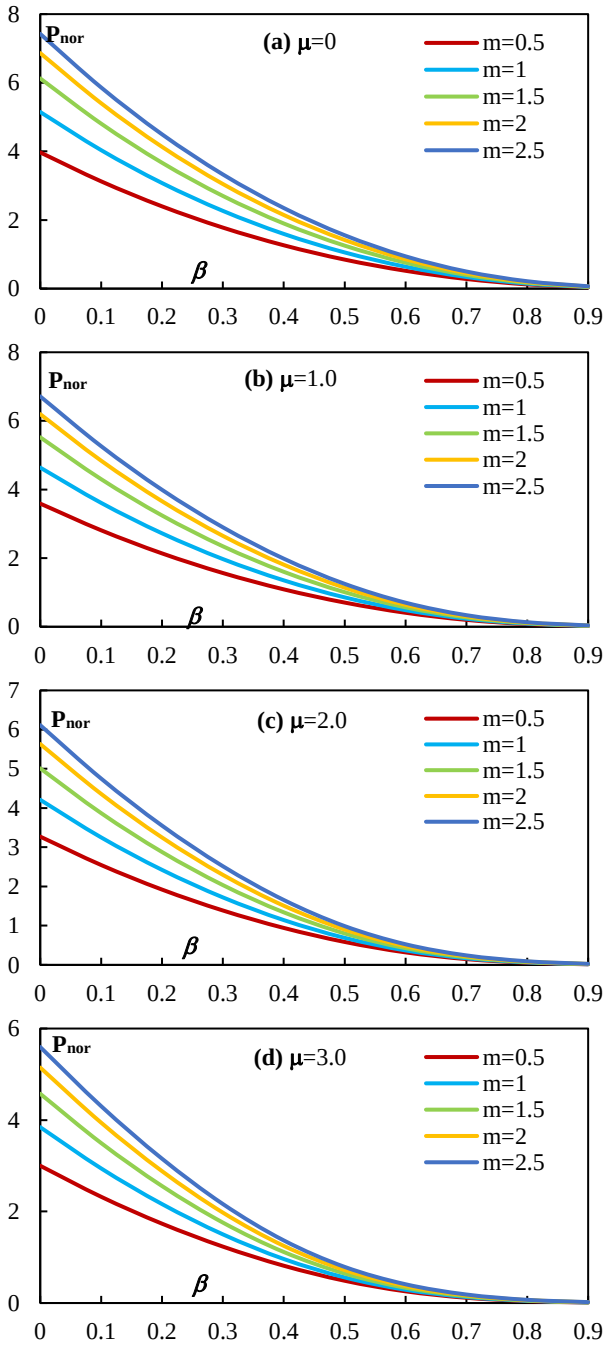

Fig. 4: Variation of the non-dimensional buckling load of tapered nanobeam with tapering ratios and power-law exponents for different nonlocality parameters (***L/b₀*=10**).

Afterward, assuming that the aspect ratio is equal to 20, Fig. 5 illustrates the contour plots of the non-dimensional buckling load for homogenous member resting on Winkler foundation with respect to the tapering ratio (β) and Winkler parameter ($\bar{k}_w$) for local beam (μ=0) and nanobeam (μ=2). Corresponding outcomes for AFG beam with m=2 are presented in Fig. 6.

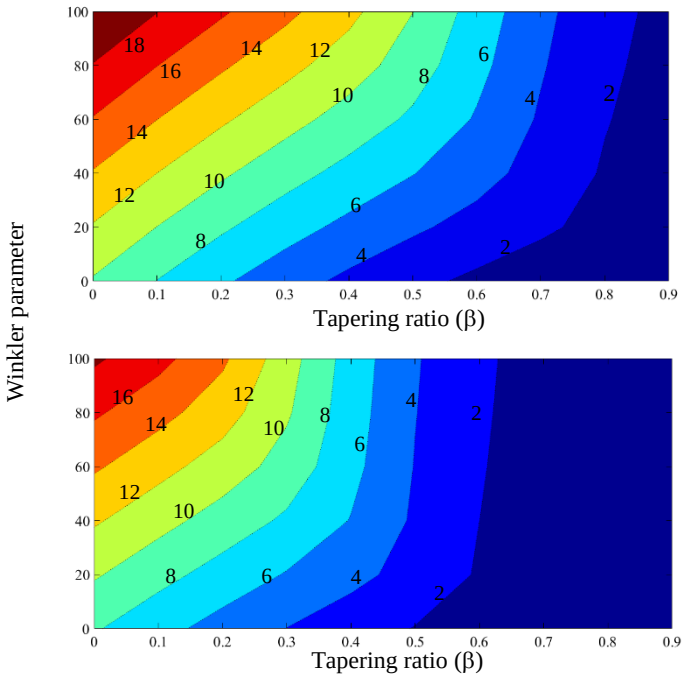

Fig. 5: Contour plot of buckling load with respect to tapering ratio (β) and Winkler parameter ($\bar{k}_w$) for homogenous beam made from Alumina (a) μ=0, (b) μ=2

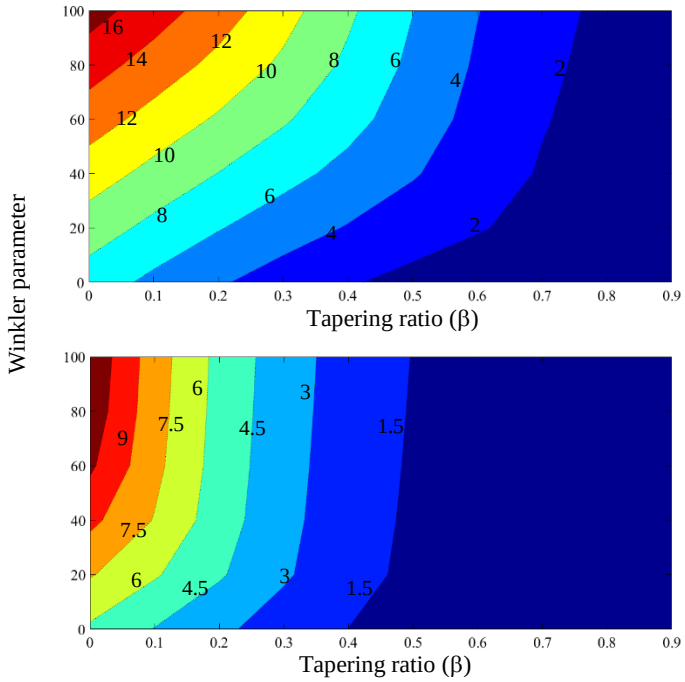

Fig. 6: Contour plot of buckling load with respect to tapering ratio (β) and Winkler parameter ($\bar{k}_w$) for AFG beam with m=2 (a) μ=0, (b) μ=2

Next, the magnitude of the normalized buckling parameter (P_{nor}) for various tapering ratios, Winkler's parameters, nonlocal parameters (μ= 0, 0.5 and 0.75) with three different values of in-homogenous index (m=0.6, 1.2 and 1.8) at ***L/b₀*=10** is listed in Table 3.

[DOR: 20.1001.1.23454296.2018.3.2.5.3]
[DOI: 10.29252/nmce.3.2.35]

Table 3: Power-law exponent, Winkler parameter and tapering ratio effects on the normalized buckling load (P_{nor}) of simply supported Timoshenko nanobeam with different nonlocal parameters (L/b_0=**10**).

Nonlocal Parameter	Winkler Parameter	Normalized buckling load (P_{nor})								
		m=0.6			**m=1.2**			**m=1.8**		
		β=0	**β=0.3**	**β=0.6**	**β=0**	**β=0.3**	**β=0.6**	**β=0**	**β=0.3**	**β=0.6**
μ=0	$\bar{k}_w = 0$	4.215	1.882	0.549	5.599	2.475	0.704	6.629	2.948	0.839
	$\bar{k}_w = 10$	5.202	2.800	1.273	6.584	3.385	1.426	7.618	3.863	1.568
	$\bar{k}_w = 30$	7.163	4.543	2.190	8.542	5.132	2.456	9.589	5.635	2.674
μ=0.5	$\bar{k}_w = 0$	4.002	1.762	0.486	5.312	2.307	0.617	6.292	2.748	0.733
	$\bar{k}_w = 10$	4.983	2.650	1.064	6.288	3.181	1.196	7.275	3.628	1.323
	$\bar{k}_w = 30$	6.924	4.244	1.559	8.224	4.784	1.776	9.227	5.265	1.973
μ=0.75	$\bar{k}_w = 0$	3.903	1.706	0.458	5.177	2.229	0.577	6.135	2.654	0.685
	$\bar{k}_w = 10$	4.880	2.576	0.961	6.150	3.081	1.084	7.114	3.511	1.204
	$\bar{k}_w = 30$	6.809	4.064	1.336	8.072	4.580	1.524	9.055	5.051	1.700

Firstly, it is important to mention that the classical isotropic beam theory is obtained by setting the nonlocal parameter and AFG power-index to zero ($\mu=m=0$).

It is observable from these illustrations that for both local and nonlocal beams and all values of non-uniformity ratio, as AFG power index (***m***) increases the stability strength enhances. In other words, a higher buckling capacity is obtained with the increment of the power index. The reason is the higher portion of the ceramic phase as the value of the gradient index rises. It can also be interpreted from Fig. 4 that for $0.5 \le m \le 1.5$, the non-dimensional critical loads increase significantly whereas, for m>1.5, the buckling capacity increases slightly and approaches maximum magnitude.

The tables and figures indicate that the non-uniformity parameter (β) has a noticeable impact on the non-dimensional buckling loads. According to the illustrations, it is found out that the buckling capacity decrease with an increase in the tapering ratio. Additionally, it is revealed that the normalized buckling load enhances with the increase in aspect ratio due to decreasing the influence of shear deformation. For more information please see [40].

As seen in Figs. 5 and 6 as well as Table 3, the buckling load increases as Winkler parameter increases. It is also deduced that the influence of Winkler foundation on the buckling capacity of local beams and nonlocal ones is different. For example, in the case of AFG nanobeams (Fig. 6b), the normalized buckling load does not increase with the increment of Winkler parameter for β>0.5. However, this behavior is seen for β>0.7 in the case of the conventional Timoshenko beam made of FGMs (Fig. 6a). Eventually, it can be stated the impact of elastic foundation on the stability of Timoshenko beam based on the classical continuum model and the nonlocal theory is more pronounced for a smaller rate of cross-section change. By comparing Fig. 6a and Fig. 6b, it is also observed the dimensionless buckling load reduces sharply for local Timoshenko beam as the tapering ratio (β) increases contrasting to Timoshenko nanobeam and the reduction is more noticeable for higher values of Winkler parameter.

As expected, for all analyzed cases, the nonlocal parameter shows a stiffness–softening effect and reduces the buckling strength. The display results in Figs. 2-6 and Table 3 also reveal that the descendent effect of Eringen's nonlocal parameter on non-dimensional buckling loads is more observable for larger values of tapering ratio and gradient indexes, especially uniform beams made of pure ceramic. This statement can be explained by the fact that the flexural stiffness of simply supported tapered beam with the nonlocal theory is inversely proportional to the Eringen's parameter. In general, the inclusion of the nonlocal effect increases the deflection, which in turn leads to a noticeable decrease in the value of the stiffness and rigidity of the member and consequently a weaker member is obtained. Since the linear buckling resistance of the beam is directly proportional to the stiffness of the member, a significant decrease in the critical load of the beam is thus observed.

5. Conclusions

In this paper, the nonlocal stability analysis of tapered Timoshenko nanobeams with axially varying material properties supported by the continuum Winkler foundation was assessed within the framework of first-order shear deformation theory and nonlocal elasticity theory. In this regard, the two couple equilibrium equations in terms of

[DOR: 20.1001.1.23454296.2018.3.2.5.3]
[DOI: 10.29252/nmce.3.2.35]

vertical and rotation displacement and related boundary conditions are established using the energy method.

The buckling capacity of Timoshenko nanobeam under simply supported end conditions was assessed, regarding this, the impacts of various parameters such as nonlocal parameter, tapering ratio, gradient index, Winkler foundation modulus, and length to thickness ratio were exhaustively discussed. According to the obtained numerical outcomes, it is concluded that the mentioned above parameters play significant roles in stability strength of AFG nanobeams. It is illustrated that the non-dimensional buckling load increases with the increase in the percentage of the ceramic phase. Additionally, it is revealed that the increase in Eringen's parameter leads to decrease the buckling strength. It is also deduced that the increment of Winker parameter and aspect ratio enhances the normalized buckling load. It can be stated the impact of elastic foundation on stability of Timoshenko beam based on the classical continuum model and the nonlocal theory is more pronounced for a smaller rate of cross-section change.

References

[1] Yang FA, Chong AC, Lam DC, Tong P. Couple stress based strain gradient theory for elasticity. International Journal of Solids and Structures. 2002; 39(10):2731-43.

[2] Gurtin ME, Weissmüller J, Larche F. A general theory of curved deformable interfaces in solids at equilibrium. Philosophical Magazine A. 1998; 78(5):1093-109.

[3] Eringen AC. Nonlocal polar elastic continua. International journal of engineering science. 1972; 10(1):1-6.

[4] Eringen AC. On differential equations of nonlocal elasticity and solutions of screw dislocation and surface waves. Journal of Applied Physics, 1983; 54: 4703-4710.

[5] Elishakoff I, Guede Z. Analytical polynomial solutions for vibrating axially graded beams. Mechanics of Advanced Materials and Structures. 2004; 11(6):517-33.

[6] Reddy JN. Nonlocal theories for bending, buckling and vibration of beams. International Journal of Engineering Science. 2007; 45(2-8):288-307.

[7] Wang CM, Zhang YY, He XQ. Vibration of Non-local Timoshenko Beams. Nanotechnology 2007; 18: 1–9.

[8] Aydogdu M. A general nonlocal beam theory: its application to nanobeam bending, buckling and vibration. Physica E: Low-dimensional Systems and Nanostructures. 2009; 41(9):1651-5.

[9] Civalek Ö., Akgöz B. Free vibration analysis of microtubules as cytoskeleton components: nonlocal Euler-Bernoulli beam modeling. Scientia Iranica-Transaction B: Mechanical Engineering, 2010; 17(5): 367-375.

[10] Danesh, M., Farajpour, A., Mohammadi, M., Axial vibration analysis of a tapered nanorod based on nonlocal elasticity theory and differential quadrature method. Mechanics Research Communications, 2012; 39(1): 23-27.

[11] Wang, B.L., Hoffman, M. and Yu, A.B., 2012. Buckling analysis of embedded nanotubes using gradient continuum theory. Mechanics of Materials, 45, pp.52-60.

[12] Eltaher MA, Alshorbagy AE, Mahmoud FF. Determination of neutral axis position and its effect on natural frequencies of functionally graded macro/nanobeams. Composite Structures. 2013; 99:193-201.

[13] Eltaher MA, Emam SA, Mahmoud FF. Static and stability analysis of nonlocal functionally graded nanobeams. Composite Structures. 2013; 96:82-8.

[14] Akgöz B, Civalek Ö. Free vibration analysis of axially functionally graded tapered Bernoulli–Euler microbeams based on the modified couple stress theory. Composite Structures, 2013; 98: 314-322.

[15] Ke LL, Wang YS. Free vibration of size-dependent magneto-electro-elastic nanobeams based on the nonlocal theory. Physica E: Low-Dimensional Systems and Nanostructures. 2014; 63:52-61.

[16] Pandeya A, Singhb J. A variational principle approach for vibration of non-uniform nanocantilever using nonlocal elasticity theory. Proced. Mater. Sci. 2015; 10: 497-506.

[17] Shafiei N, Kazemi M, Safi M, Ghadiri M. Nonlinear vibration of axially functionally graded non-uniform nanobeams. International Journal of Engineering Science, 2016; 106: 77-94.

[18] Akgöz, B. and Civalek, Ö. 2016. Bending analysis of embedded carbon nanotubes resting on an elastic foundation using strain gradient theory. Acta Astronautica, 119, pp.1-12.

[19] Ghasemi, A.R. and Mohandes, M., 2016. The effect of finite strain on the nonlinear free vibration of a unidirectional composite Timoshenko beam using GDQM. Advances in aircraft and spacecraft science, 3(4), p.379.

[20] Mohandes, M. and Ghasemi, A.R., 2016. Finite strain analysis of nonlinear vibrations of symmetric laminated composite Timoshenko beams using generalized differential quadrature method. Journal of Vibration and Control, 22(4), pp.940-954.

[21] Ebrahimi F, Salari E. Nonlocal thermo-mechanical vibration analysis of functionally graded nanobeams in thermal environment, Acta Astronautica, 2015; 113: 29-50.

[22] Ebrahimi F, Barati M R. Buckling analysis of nonlocal third-order shear deformable functionally graded piezoelectric nanobeams embedded in elastic medium, J. Brazil. Soc. Mech. Sci. Eng. 2016; 39(3); 937-952.

[23] Ebrahimi F, Barati M R. A nonlocal strain gradient refined beam model for buckling analysis of size-dependent shear-deformable curved FG nanobeams, Compos. Struct. 2017; 159: 174-182.

[24] Mercan, K. and Civalek, Ö, 2016. DSC method for buckling analysis of boron nitride nanotube (BNNT) surrounded by an elastic matrix. Composite Structures, 143, pp.300-309.

[25] Calim, F.F., 2016. Free and forced vibration analysis of axially functionally graded Timoshenko beams on two-parameter viscoelastic foundation. Composites Part B: Engineering, 103, pp.98-112.

[26] Lezgy-Nazargah, M., Vidal, P. and Polit, O., 2013. An efficient finite element model for static and dynamic analyses of functionally graded piezoelectric beams. Composite Structures, 104, pp.71-84.
[27] Lezgy-Nazargah, M. and Farahbakhsh, M., 2013. Optimum material gradient composition for the functionally graded piezoelectric beams. International Journal of Engineering, Science and Technology, 5(4), pp.80-99.
[28] Lezgy-Nazargah, M., 2015. A three-dimensional exact state-space solution for cylindrical bending of continuously non-homogenous piezoelectric laminated plates with arbitrary gradient composition. Archives of Mechanics, 67(1), pp.25-51.
[29] Lezgy-Nazargah, M., 2016. A three-dimensional Peano series solution for the vibration of functionally graded piezoelectric laminates in cylindrical bending. Scientia Iranica. Transaction A, Civil Engineering, 23(3), p.788.
[30] Lezgy-Nazargah, M., 2015. Fully coupled thermo-mechanical analysis of bi-directional FGM beams using NURBS isogeometric finite element approach. Aerospace Science and Technology, 45, pp.154-164.
[31] Lezgy-Nazargah, M. and Meshkani, Z., 2018. An efficient partial mixed finite element model for static and free vibration analyses of FGM plates rested on two-parameter elastic foundations. Struct Eng Mech, 66, pp.665-676.
[32] Demir C, Mercan K, Numanoglu H M, Civalek Ö. Bending response of nanobeams resting on elastic foundation. J. Appl. Comput. Mech. 2018; 4(2): 105-11.
[33] Soltani, M. and Mohammadi, M., 2018. Stability Analysis of Non-Local Euler-Bernoulli Beam with Exponentially Varying Cross-Section Resting on Winkler-Pasternak Foundation. Journal of Numerical Methods in Civil Engineering, 2(3), pp.67-77.
[34] Ghannadiasl, A., 2019. Natural frequencies of the elastically end restrained non-uniform Timoshenko beam using the power series method. Mechanics Based Design of Structures and Machines, 47(2), pp.201-214.
[35] Soltani, M. and Asgarian, B., 2019. New hybrid approach for free vibration and stability analyses of axially functionally graded Euler-Bernoulli beams with variable cross-section resting on uniform Winkler-Pasternak foundation. Latin American Journal of Solids and Structures, 16(3).
[36] Ghasemi, A.R. and Mohandes, M., 2019. A new approach for determination of interlaminar normal/shear stresses in micro and nano laminated composite beams. Advances in Structural Engineering, 22(10), pp.2334-2344.
[37] Arefi, M. and Civalek, O., 2020. Static analysis of functionally graded composite shells on elastic foundations with nonlocal elasticity theory. Archives of Civil and Mechanical Engineering, 20(1), pp.1-17.
[38] Soltani, M. and Asgarian, B., 2020. Lateral-Torsional Stability Analysis of a Simply Supported Axially Functionally Graded Beam with a Tapered I-Section. Mechanics of Composite Materials, pp.1-16.
[39] Bellman R. E, Casti J., "Differential quadrature and long-term integration." Journal of Mathematical Analysis and Applications; 34, 235-238 (1971).
[40] Soltani M. Finite element modelling for buckling analysis of tapered axially functionally graded Timoshenko beam on elastic foundation. Mechanics of Advanced Composite Structures, DOI: 10.22075/MACS.2020.18591.1223.